

Curie temperature enhancement of electron doped $\text{Sr}_2\text{FeMoO}_6$ perovskites studied by photoemission spectroscopy

J. Navarro and J. Fontcuberta

Institut de Ciència de Materials de Barcelona Campus U.A.B., Bellaterra 08193, Catalunya, Spain

M. Izquierdo, J. Avila and M. C. Asensio

LURE, Centre Universitaire Paris-Sud, Bât. 209D, B.P. 34, 91405 Orsay Cedex, France and

Instituto de Ciencia de Materiales, CSIC, 28049 Madrid, Spain

(Dated: October 29, 2018)

We report here on the electronic structure of electron-doped half-metallic ferromagnetic perovskites such $\text{Sr}_{2-x}\text{La}_x\text{FeMoO}_6$ ($x=0-0.6$) as obtained from high-resolved valence-band photoemission spectroscopy (PES). By comparing the PES spectra with band structure calculations, a distinctive peak at the Fermi level (E_F) with predominantly $(\text{Fe}+\text{Mo}) t_{2g}^\downarrow$ character has been evidenced for all samples, irrespectively of the x values investigated. Moreover, we show that the electron doping due to the La substitution provides selectively delocalized carriers to the t_{2g}^\downarrow metallic spin channel. Consequently, a gradual rising of the density of states at the E_F has been observed as a function of the La doping. By changing the incoming photon energy we have shown that electron doping mainly rises the density of states of Mo parentage. These findings provide fundamental clues for understanding the origin of ferromagnetism in these oxides and shall be of relevance for tailoring oxides having still higher T_C .

PACS numbers: 79.60.-i, 71.45.Lr, 64.60.-i, 73.20.At

I. INTRODUCTION

The early discovery of colossal magnetoresistance (CMR) has abundantly stimulated the research on manganese oxides because of their leading technologic applications, not counting their critical importance in basic physics. However, typically the magnetoresistance strength diminishes as T_C increases up to room temperature, thus making it difficult the direct technologic use of these advanced materials. As progress of spintronics requires fully spin-polarized ferromagnetic materials, having Curie temperatures (T_C) well above room temperature, recent finding of room-temperature tunneling magnetoresistance and half-metallic (HM) behavior of $\text{Sr}_2\text{FeMoO}_6$ (SFMO) oxides with $T_C \sim 400\text{K}^1$ has opened renewed interest and expectative for promising applications. $\text{A}_2\text{MM}'\text{O}_6$ double perovskites are built up by alternate $\text{M}'\text{O}_6$ and MO_6 octahedral units bonded by oxygen bridges, where A is an alkaline earth or rare-earth ion and M, M' are 3d and 4d/5d transition metals. These novel materials are predicted to be $\text{HM}^{1,2,3,4}$, where the metallic behavior of one electron spin channel is coexisting with an energy gap between valence and conduction bands for electrons of the other spin polarization. In short, the electronic configuration of SFMO can be described by $\text{Fe}(3d^{6-\delta}):\text{Mo}(4d^\delta)$ ($\delta=0.3^5$). The Fe-3d full-filled (t_{2g}^3 and e_g^2) *spin-up* electrons can be viewed as localized whereas the Fe 3d partially empty ($t_{2g}^{1-\delta}$) *spin-down* states are strongly hybridized with O-2p orbitals and partially empty Mo-4d $^\delta$ (*spin-down*) states. Consequently, these transition-metal oxides alloys present bands associated to one spin polarization (in this case Fe-3d *spin-up*) entirely filled, which are separated from unoccupied bands of the same symmetry by a bandgap

sited at the Fermi level. Whereas, the other spin channel involving Fe-3d and Mo-4d *spin-down* electrons has a metallic character.

Recent photoemission spectroscopy (PES) experiments^{6,7,8} have provided evidence of the half metallic character of SFMO by determining that the states close to the Fermi level have predominantly Mo t_{2g}^\downarrow and Fe t_{2g}^\downarrow character. By comparing photon-energy dependence of the valence band spectra and the local spin-density approximation (LSDA) band structure theoretical calculations has revealed that the delocalized electrons at the E_F are totally *spin-down* polarized. Consistent results have been lately obtained by using X-ray absorption spectroscopy (XAS) experiments⁹. The site-specific reported information is also in agreement with LSDA theoretical calculations that contemplate well-localized t_{2g}^3 and e_g^2 *spin-up* Fe-3d sub-bands are well below the Fermi level and that the delocalized t_{2g} *spin-down* sub-bands due to the Mo(4d) and Fe (3d) are at the E_F . These spectroscopic results together with recent magnetic measurements in the paramagnetic phase¹⁸ support that the AFM interaction is driven by a mechanism where the itinerant carriers and the Fe localized cores tend to be antiparallel, at variance with the double exchange interaction.

Magnetic measurements are consistent with ferromagnetic ordering of $\text{Fe}(3d^{6-\delta})$ moments which shall be antiferromagnetically coupled to any moment on $\text{Mo}(4d^\delta)$ sites. Understanding of the physical mechanism lying behind the ferromagnetic ordering remains challenging. Difficulties arise mainly due to the fact that in this structure the 4d(Mo) ions are essentially non-magnetic and thus the separation between the magnetic ions (3d(Fe)) is substantially large ($\sim 8 \text{ \AA}$). In spite of this, the Curie

temperature is very high, exceeding that of the celebrated manganites ($T_C < 360\text{K}$). This observation suggests that the Double Exchange model used to describe the ferromagnetism in manganites cannot be safely used in the present case. Sarma et al.⁶ proposed that due to the Fe-Mo hybridization, the intra-atomic exchange in Mo is much enhanced thus resulting in a strong antiferromagnetic coupling between Fe and Mo and thus the leading to an effective more robust Fe-Fe ferromagnetic ordering. Recently, Fang et al.¹⁰ have proposed that ferromagnetism is stabilized by the exchange splitting of the Mo(4d) orbitals, which lowers the energy of carriers and promotes a charge transfer from the *spin-up* to the *spin-down* subbands.

Based on neutron diffraction^{1,11,12} and early Mössbauer spectroscopy data¹³, ferrimagnetism was proposed to be originated from the AFM ordering of Fe^{3+} ($3d^5$; $t_{2g}^3 e_g^2$): Mo^{5+} ($4d^1$; t_{2g}^1) configurations, thus predicting a saturation magnetization of $4\mu_B$. However, the experimental values of the saturation moment is commonly found to be of about $3.1\text{--}3.2\mu_B$ ^{1,13,14,15}. So far, this sensible diminution of the saturation moment has been attributed to a partial Fe-Mo disorder. From more recent Mössbauer data, however, a state of valence-fluctuation of $\text{Fe}^{2.5+}$ has been proposed by Lindén et al.¹⁶ and Balcells et al.⁵, and this has been sustained by Chmaissen et al. who has found $\mu_{Fe}=4.3\text{--}4.4\mu_B$ from a simultaneously study based on neutron diffraction and Mössbauer techniques¹⁷. We recall that, as indicated in⁵, the saturation magnetization values can not allow discriminating among Fe^{3+} : Mo^{5+} or Fe^{2+} : Mo^{6+} electronic configurations. The effective moment in the paramagnetic phase shall be insensitive to the presence of Fe/Mo disorder and should, in principle, to allows discrimination between Fe^{3+} : Mo^{5+} or Fe^{2+} : Mo^{6+} configurations, thus it may provide a more robust insight into the electronic configuration of the Fe/Mo ionic species. Using this approach, Tovar et al.¹⁸ have recently shown that the magnetic properties in the paramagnetic regime cannot be understood by considering only the contribution of localized moments: the effective paramagnetic moment is found to be smaller that it should be expected for any electronic configuration Fe ($3d^6$):Mo($4d^0$) or Fe($3d^5$):Mo($4d^1$)¹⁹.

In fact, the paramagnetic susceptibility data has been modeled¹⁸ by assuming that there is an exchange induced spin polarization of the conduction band being antiferromagnetically coupled to the localized moments by Hund coupling. Even more, the strength of the ferromagnetic coupling has been predicted to be proportional to the density of states at the Fermi level ($D(E_F)$). These findings may provide microscopic understanding of the observed augmentation of the Curie temperature upon electron doping²⁰ although direct evidence is still lacking. Similarly, evidence of a half-metallic ferromagnetic nature of these electron-doped double perovskites is still missing.

Here, we report on synchrotron radiation pho-

toemission measurements near the Fermi level of $\text{Sr}_{2-x}\text{La}_x\text{FeMoO}_6$ with a gradual level of electron doping. As it has been recently shown²⁰, the doping (achieved via partial substitution of Sr^{+2} by La^{+3}) promotes a substantial enhancement of the Curie temperature (with ΔT_C up to 80K). These experimental evidences, sharply contrast with some recent predictions²¹ thus illustrating the complexity of phase diagram in double perovskites. We will show here, that as the La substitution progresses, a noticeable enhancement of the $D(E_F)$ -mainly of Mo(4d) parentage is measured. A clear correlation between $D(E_F)$ and T_C is discovered. In addition, we provide spectroscopic evidence that the electron injection supplies carriers to the metallic spin-down channel; whilst the other Fe-3d full-filled (t_{2g}^3 and e_g^2) spin-up insulating channel remains unchanged. These results constitute a stringent test for proposed models for electronic structure and ferromagnetism in SFMO and shall provide guidelines for further progress on tailoring ferromagnetic metals having optimal properties for spintronics.

II. EXPERIMENTAL DETAILS

Photoemission spectroscopy (PES) experiments on $\text{Sr}_{2-x}\text{La}_x\text{FeMoO}_6$ ceramic samples have been performed at the SU8 beamline at LURE using synchrotron radiation light between 14 till 890 eV provided by an insertion device of Super-Aco storage ring,^{22,23}. The Fermi level of the oxides have been determined using Cu as reference. In the range of explored energies $h\nu$ the energy resolution is of about 50 meV^{23,24,25}. The measured intensity has been normalized with respect to the intensity of the deep O(2p) states. Due to the polycrystalline nature of the investigated samples, the results reported here should be considered as angle-integrated data, because the lack of momentum discrimination in the reciprocal space. Sample preparation, structural and magnetic characterization can be found elsewhere^{5,19,20}. Here, in order to illustrate the high quality of the used samples, we only mention that in the pristine compound ($x=0$), the saturation magnetization is $M_S=3.8\mu_B$ and the antisite concentration (i.e. misplaced Fe/Mo ions) is $\sim 5\%$ and the Curie temperature (determined from extrapolation of the magnetization curves) is of about 430K. For the rest of samples the corresponding values are $T_C=440\text{K}$, 465K and 480K for $x=0.2$, 0.4 and 0.6 respectively. These T_C values are comparable to those reported in Ref.²⁰ for similar samples. The T_C values determined from the Arrot plots also show the same systematic rise with doping although the absolute values are somewhat lower; for instance $T_C=400\text{K}$ and 420K for $x=0$ and 0.4 respectively. Refinement of neutron diffraction profiles have been used to confirm that, within the experimental resolution, all samples here reported are oxygen stoichiometric²⁶. Samples have been scratched in situ in ultra-high vacuum ($<3 \cdot 10^{-11}$ torr) by using a diamond saw. Surface contamination has been monitored by the eventual presence of C

1s core level. All measurements have been carried out at room temperature.

III. RESULTS

Figure 1 shows the valence band spectrum of $\text{Sr}_{2-x}\text{La}_x\text{FeMoO}_6$ ($x=0, 0.2, 0.4$, and 0.6) samples collected using $h\nu=50\text{eV}$. As it has been reported before for non-electron doped samples^{7,8}, the two major features, occurring at -8 and -6 eV correspond to $\text{O}(2p)$ and $\text{Fe}(e_{2g}^\uparrow)$ states respectively. The metallic edge can be well recognized. Substantial modifications of the spectra are observed at or around ($0\text{-}2\text{eV}$) the Fermi level upon La substitution. Within the context of this paper of the greatest interest is the valence band spectrum close to the E_F as shown in Figure 2. To elucidate the origin of the observed changes in the spectra, we have recorded spectra at different photon energies with the purpose of taking advantage of the dependence of the photoionization cross sections (σ) of the different elements on the photon energy. Detailed inspection of these spectra immediately reveals a finer structure. At $h\nu=90$ eV (Fig. 2 (top)), where the cross section of the Fe electronic states is much higher than those from molybdenum and oxygen ($\sigma(\text{Fe}):\sigma(\text{Mo}):\sigma(\text{O})\sim 7:0.1:1.5$), the spectra show two main features, one state at the Fermi edge which changes slightly its intensity as the electron doping progresses and other state extended from 0.7 eV to 2.5 eV, whose intensity is unchanged as the La doping increases. In Fig. IV (middle) we show the same spectra recorded at $h\nu=50\text{eV}$, where the cross sections of Fe, Mo and O ions are comparable ($\sigma(\text{Fe}):\sigma(\text{Mo}):\sigma(\text{O})\sim 9:3.5:6$). Both features are present; however their behavior as a function of doping is different: in this case, the intensity of both states is clearly rising as the La content increases, thus revealing a gradual modifications of Mo and O derived states. We include in Figure 2 (bottom) the theoretical density of states for the parent compound as recently calculated by Saitoh et al⁸. In agreement with computations^{1,4,8,10}, we note that the experimental features observed in the PES can be assigned to: oxygen $\text{O}(2p)$ hybridized spin-up $\text{Fe}(e_g)$ (-1 to -2.5 eV) states and spin-down $\text{Fe}(t_{2g})+\text{Mo}(t_{2g})$ states (0 to -1 eV).

Deconvolution of the experimental data has been done (Fig. 3) using a background gaussian function that collects the tail of the -6 eV peak (Fig. 2) plus three gaussian peaks, labeled C, B and A convoluted with the Fermi function in Fig. 3. The solid line through the data shows the quality of fits. This decomposition allows a clear identification of the states (B at ~ -2.0 eV and C at ~ -1.25 eV), corresponding to the spin-up $\text{Fe}(e_g)$ doublet band predicted by several theoretical works^{1,2,3,4,6,7,8,10}. The expected theoretical band width of 1.5 eV for the spin-up $\text{Fe}(e_g^\uparrow)$ states agrees quite well with the states labeled as B and C. Taking into account the spectral weight broadening due to the relative high measurement temperature, we can estimate the photoemission half-gap on the occu-

pled state side of the majority spin-up $\text{Fe}(e_g^\uparrow)$ channel to be $0.7\pm 0.2\text{eV}$. The peak labeled A, extending up to the Fermi level, can be associated to spin-down $\text{Fe}(t_{2g}^\downarrow)$ and $\text{Mo}(t_{2g}^\downarrow)$ states. The comparison of the PES spectra with theoretical predictions^{1,8} shown in Fig. 2 confirms the peak assignation we have made. From data in Fig. 2, it is clear that the position of the spin-up $\text{Fe}(e_g^\uparrow)$ states (B and C), does not change noticeably with La doping, indicating that the spin-up (majority) channel gap is not perturbed by the electron injection all along the investigated doping regime.

It is important to notice that, in agreement with recent predictions²¹, the results shown in Fig. 3 indicate that a simple rigid-band model cannot be used to analyze the data. In this framework, it shall be expected that a charge transfer or carrier doping may promote a rigid upward shift of the Fermi level in order to fill with the extra charge *available unoccupied bands*. If this were the case the binding energy of both spin channels should have been increased in the same amount as the Fermi level may have been shifted. In spite of this, only the states at the Fermi level (feature A of Fig. 2) associated to the delocalized spin-down Mo states are modified. The spectral weight related to those totally polarized states increases and their binding energy shifts slightly away from the Fermi level. In contrast, features B and C associated to the spin-up channel are not affected by the electron doping keeping their binding energy unchanged for different La content. Consequently, the photoemission half-gap on the occupied state side of the minority spin-up $\text{Fe}(e_g^\uparrow)$ channel remains invariable ($< 0.7\pm 0.2\text{eV}$) irrespectively on doping.

In order to determine the origin of the progressive rising of the intensity of peaks A, B and C, we concentrate our analysis on the PES spectra (Fig.2) obtained at the Mo Cooper minimum ($h\nu=90$ eV), with purpose to discriminate the relative contribution of the Fe and Mo to the corresponding states. Top part of Fig. 2 reveals that at $h\nu=90$ eV the t_{2g}^\downarrow states do not change their intensity upon La doping, thus indicating that the enhancement observed at $h\nu=50$ eV is due to the some progressive admixture of Mo (A) and oxygen hybridized orbitals (B and C), to the bottom of the conduction and top of the valence band respectively. Of fundamental importance is the observation that at $h\nu=50\text{eV}$ (and to lower extent also for $h\nu=90$ eV) the intensity of the t_{2g}^\downarrow peak (labeled A) increases and thus the corresponding density of states at the Fermi level $D(E_F)$ also rises. This is a key result that reveals that La doping and the accompanying electron injection promote an enhancement of $D(E_F)$. The fact that this effect is almost canceled when photons insensitive to Mo states are used, suggests that the electron doping supplies charge almost exclusively to previously unoccupied spin down \downarrow Mo states, although these states may be strongly hybridized with oxygen and Fe states.

The density of states $D(E_F)$ has been evaluated by integrating the measured PES intensity measured at 50

eV (Fe and Mo sensitive, Fig. 2(middle) over an energy range of ± 100 meV around the Fermi edge inflexion point. As shown in Figure 4 (inset), where we collect the normalized $D(E_F)$ vs La concentration (x) (solid circles), there is a roughly linear enhancement of $D(E_F)$ upon doping. We have tested the robustness of this result by integrating the PES intensity over other energy ranges (50-200 meV). No significant variation of the $D(E_F, x)$ dependence is found. The relevance of this finding can be better appreciated in Fig. 4 (main panel) where we plot the $D(E_F)$ values together with the Curie temperature of each $\text{Sr}_{2-x}\text{La}_x\text{FeMoO}_6$ sample. A striking, almost linear, dependence of T_C on the $D(E_F)$ is obtained. This is a fundamental result that reveals and illustrates the role of the itinerant carriers on the ferromagnetic coupling in these oxides. The prediction that T_C may rise when increasing the $D(E_F)$ contained in the formalism of analysis of effective moment and ferromagnetic coupling recently developed by Tovar et al.¹⁸ was at the heart of the attempts to rise T_C by electron doping²⁰. It is worth to notice that the density of states projected on the Fe state, as determined from the PES obtained at $h\nu=90$ eV (open circles in Fig. 4 (inset)), does not show any significant variation upon La doping thus illustrating that doping carriers occupy mainly Mo orbitals.

The data shown here do not provide insight into the microscopic mechanism for the modification of the density of states, although it is clearly triggered by the La doping. The difficulty arises due to the fact that the carrier injection associated to the La doping is accompanied by a gradual cell expansion and structural distortion and the enhanced presence of antisites²⁰. These effects are the result of the different sizes of La/Sr ions and a reduced driving force for Fe/Mo ordering due to the electron injection. The latter would be consistent with doping electrons occupying Mo-4d orbitals²¹ and thus in agreement with the present data. The former may reduce the Mo-O-Fe orbital overlapping thus shrinking the

conduction band. However, to what extent these phenomena contribute to the observed modifications of the $D(E_F)$ is nowadays unknown and further efforts to discriminate between bond bending, antisites and genuine carrier doping are required to address this issue.

IV. CONCLUSIONS

In summary, we have provided evidenced that, in double perovskites, there is a close connection between the $D(E_F)$ and the strength of the ferromagnetic coupling and thus the Curie temperature. This experimental observation should provide a solid guide for research of half-metallic ferromagnetic oxides having still higher T_C and consequently opportunities for further developments of materials for spintronics. We shall mention that recent findings in ferromagnetic diluted semiconductors²⁷ also fit in the framework and methodologies developed here and thus the present results may have impact in areas of major current activity. On the other hand, W. Pickett²⁸ recently proposed that $\text{A}_2\text{MM}'\text{O}_6$ oxides could be ideal candidates for searching exotic spin-compensated half-metallic antiferromagnetism and eventually single spin superconductivity. Our observation that the spin-down carrier density can be adjusted by appropriate doping may provide an alternative way to reach the required fully spin compensation.

Acknowledgments

We thank the AMORE (CEE), LURE, MAT 1999-0984-CO3 and MAT 2002-03431 projects for financial support and the MCYT-LURE for making available the synchrotron radiation light.

-
- ¹ K.-I. Kobayashi et al., Nature 395, 677 (1998)
 - ² K.-I. Kobayashi et al., Phys. Rev. B 59, 11159 (1999)
 - ³ W.E. Pickett and D.J. Singh, Phys. Rev. B 53, 1146 (1996), and references therein.
 - ⁴ H. Wu, Phys. Rev. B 64, 125126 (2001)
 - ⁵ Ll. Balcells et al, Appl. Phys. Lett. 78, 781 (2001); J.M. Greneche et al, Phys. Rev. B 63, 174403 (2001)
 - ⁶ D.D. Sarma et al., Phys. Rev. Lett. 85, 2549, (2000); Z. Fang, K. Terakura and J. Kanamori, Phys. Rev. B 63, 180407(R), (2001)
 - ⁷ J.-S. Kang et al., Phys. Rev. B 64, 024429 (2001)
 - ⁸ T. Saitoh et al., Phys. Rev. B 66, 35112 (2002)
 - ⁹ S. Ray, A. Kumar, D.D. Sarma, R. Cimino, S. Turchini, S. Zennaro, and N. Zerma, Phys. Rev. Lett., 87, 097204 (2001)
 - ¹⁰ Z. Fang, K. Terakura and J. Kanamori, Phys. Rev. B 63, 180407(R), (2001)
 - ¹¹ S. Nakayama, T. Nakagawa, and S. Nomura, J. Phys. Soc. Jpn. 24, 219(1968)
 - ¹² Y. Moritomo, Sh. Xu, A. Machida, T. Akimoto, E. Nishibori, M. Takata, M. Sakata, Phys. Rev. B 61, R7827(2000)
 - ¹³ S. Nakagawa, J. Phys. Soc. Jpn. 24, 806(1968)
 - ¹⁴ M. Itoh, I. Ohta, and Y. Inaguma, Mater. Sci. Eng., B 41, 55 (1996).
 - ¹⁵ Y. Tomioka, T. Okuda, Y. Okimoto, R. Kumai, K.-I. Kobayashi, and Y. Tokura, Phys. Rev. B 61, R7827(2000).
 - ¹⁶ J. Lindén et al., Appl. Phys. Lett. 76, 2925(2000)
 - ¹⁷ O. Chmaissem et al., Phys. Rev. B 62, 14197(2000)
 - ¹⁸ M. Tovar et al., Phys. Rev. B 66, 24409 (2002)
 - ¹⁹ B. Martínez et al., J. Phys. Condens. Matter 12, 10515 (2000)
 - ²⁰ J. Navarro et al, Phys. Rev. B 64, 92411 (2001)
 - ²¹ J.L. Alonso, L.A. Fernández, F. Guinea, F. Lesmes and V. Martín-Mayor. (arXiv:cond-mat/0210303) and references therein.
 - ²² Y. Huttel, F. Schiller, J. Avila, and M.C. Asensio., Phys.

FIG. 1: Valence band spectra photoemission spectra for $\text{Sr}_{2-x}\text{La}_x\text{FeMoO}_6$ ($x=0-0.6$) recorded at $h\nu=50\text{eV}$.

FIG. 2: Photoemission spectra near E_F region of $\text{Sr}_{2-x}\text{La}_x\text{FeMoO}_6$ ($x=0-0.6$) recorded at $h\nu=90\text{ eV}$ (top) and $h\nu=50\text{ eV}$ (middle). In the bottom part, theoretical calculations adapted from Ref. 29 are included

Rev. B 61, 4948 (2000).

²³ M. E. Dávila, et al, Phys. Rev. B 62, 1635 (2000)

²⁴ A. Arranz et al, Phys. Rev. B 64, 07405 (2002).

²⁵ S. Bengiό, et al, Phys. Rev. B 65, 205326 (2002)

²⁶ C. Frontera et al., in preparation

²⁷ T. Dietl, Science 287, 1019 (2000) and references therein.

²⁸ W. Pickett, Phys. Rev. Lett. 77, 3185 (1996)

FIG. 3: Upper part of the valence band spectra for $\text{Sr}_{2-x}\text{La}_x\text{FeMoO}_6$ ($x=0-0.6$), recorded at $h\nu=50\text{ eV}$. Deconvolution of different states are indicated.

FIG. 4: Curie temperature vs the density of states $D(E_F, x)$ taken at 50 eV. Inset: Normalized $D(E_F) = D(E_F, x)/D(E_F, 0)$ taken at 50 eV (●) and 90eV (○) vs the La contents.

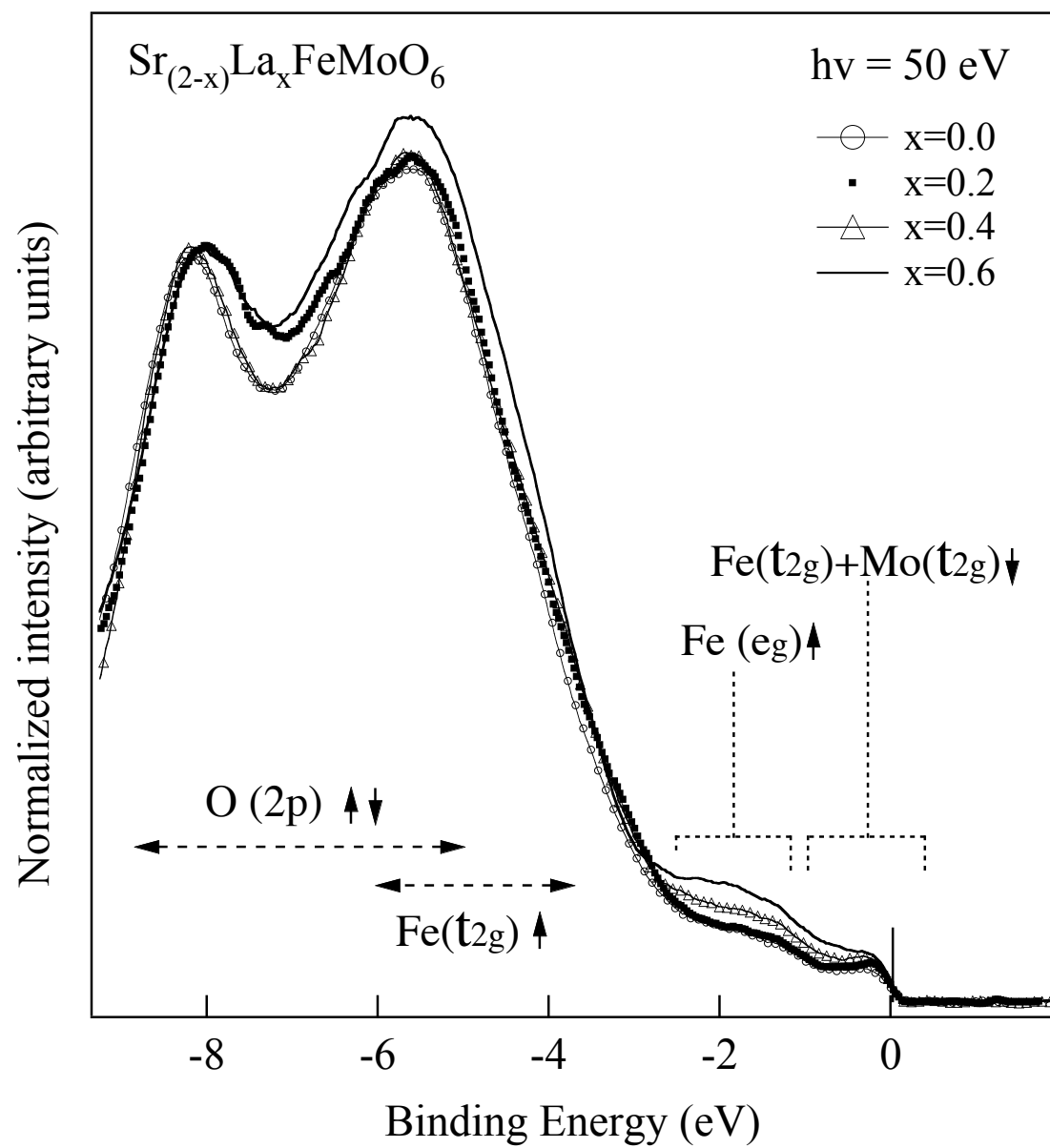


Fig 1

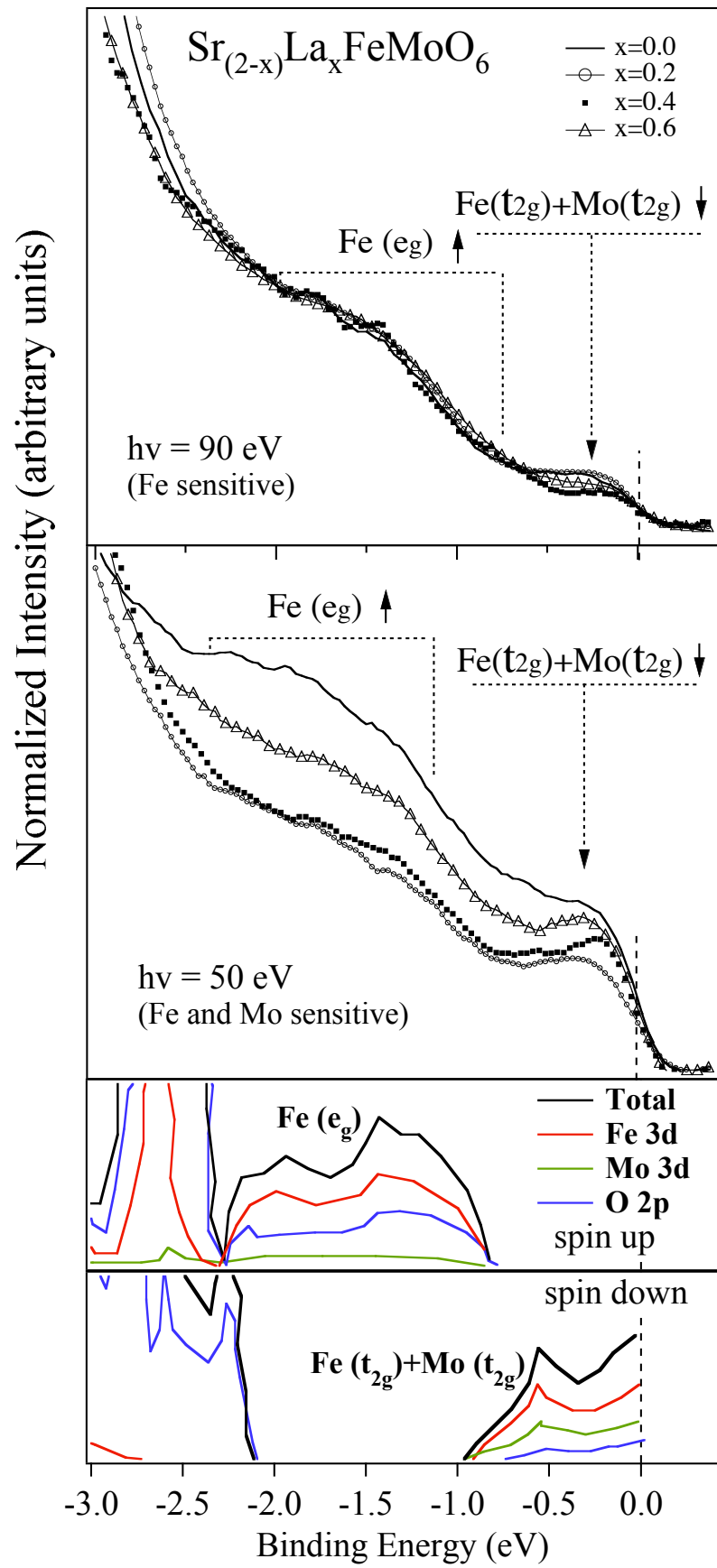


Fig 2

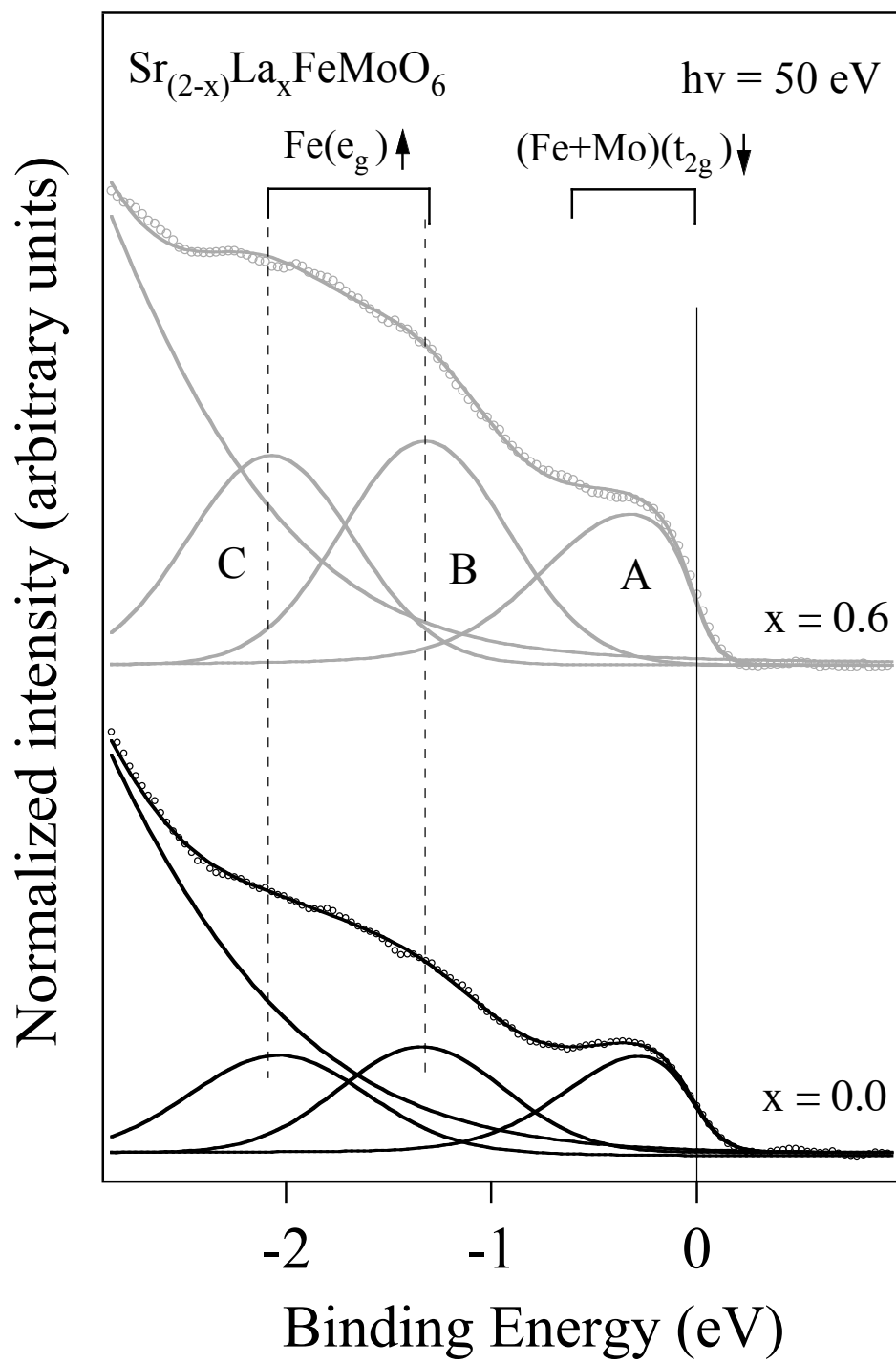


Fig. 3

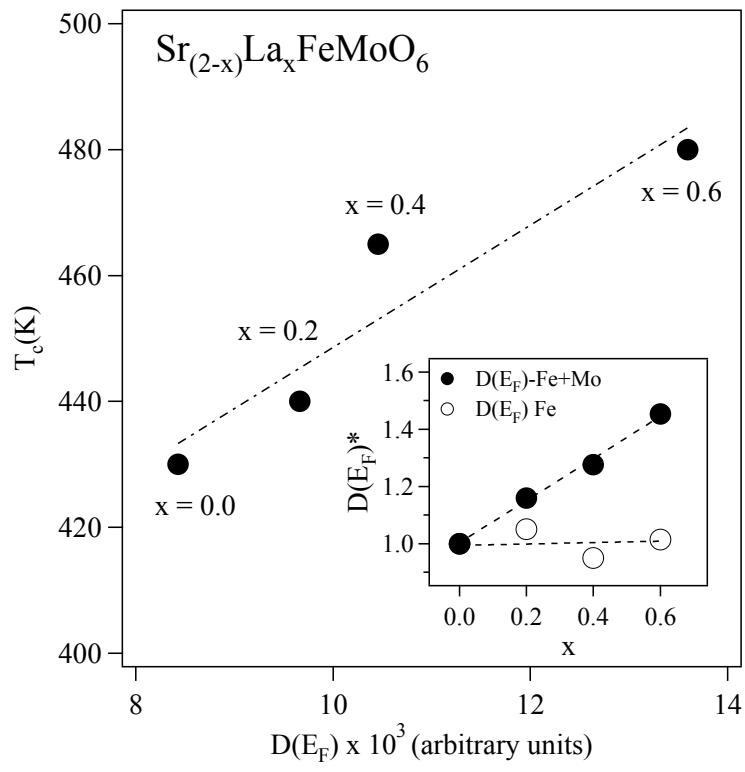


Fig 4